Cell Reports

Report

Gasdermin D mediates a fast transient release of ATP after NLRP3 inflammasome activation before ninjurin 1-induced lytic cell death

Graphical abstract

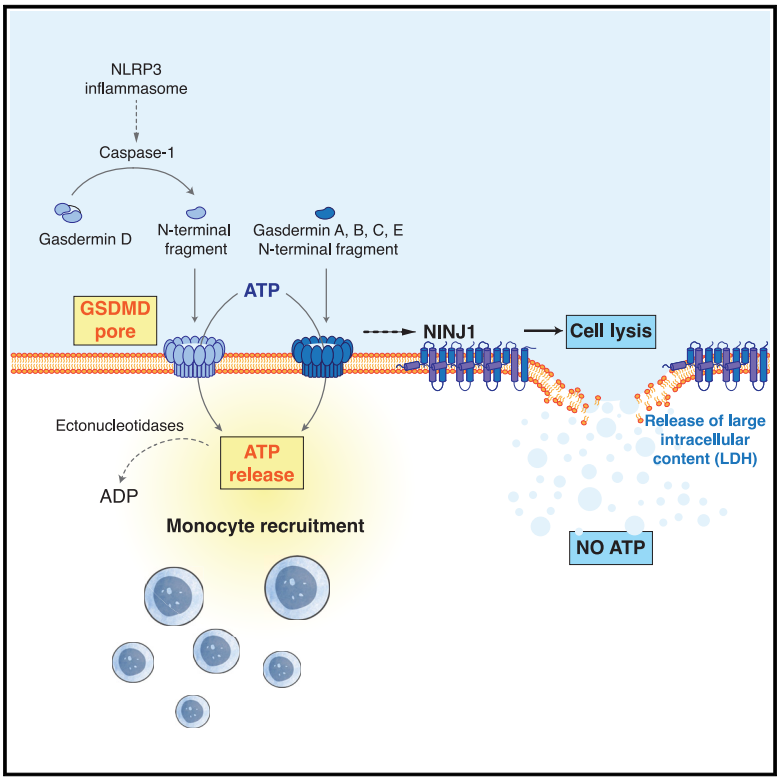

Authors

Julieta Schachter, Adriana Guijarro, Diego Angosto-Bazarra, ..., Ana B. Pérez-Oliva, Pablo J. Schwarzbaum, Pablo Pelegrin

Correspondence

julischachter@gmail.com (J.S.), pablopel@um.es (P.P.)

In brief

Schachter et al. reveal that GSDMD mediates early ATP release in macrophages during NLRP3 activation. This process occurs prior to pyroptotic cell death and is independent of NINJ1-dependent cell lysis. The released ATP drives monocyte recruitment. Other N-terminal GSDMs also increase ATP permeability, highlighting their potential role in immune modulation.

Highlights

- GSDMD mediates early ATP release in macrophages during NLRP3 activation
- ATP release occurs prior to pyroptotic cell death and is independent of NINJ1
- Monocyte migration is induced by GSDMD-dependent extracellular ATP
- N-terminal fragments of various gasdermins increase ATP permeability across cell membranes

Schachter et al., 2025, Cell Reports *44*, 115233
February 25, 2025
https://doi.org/10.1016/j.celrep.2025.115233

CellPress

Cell Reports

CellPress
OPEN ACCESS

Report

Gasdermin D mediates a fast transient release of ATP after NLRP3 inflammasome activation before ninjurin 1-induced lytic cell death

Julieta Schachter,[1,5,*] Adriana Guijarro,[2,5] Diego Angosto-Bazarra,[2] Miriam Pinilla,[2] Laura Hurtado-Navarro,[2] Etienne Meunier,[3] Ana B. Pérez-Oliva,[2] Pablo J. Schwarzbaum,[1] and Pablo Pelegrin[2,4,6,*]

[1]Department of Biological Chemistry and Institute of Biochemistry and Biophysics (IQUIFIB), School of Pharmacy and Biochemistry, University of Buenos Aires, Buenos Aires, Argentina
[2]Biomedical Research Institute of Murcia (IMIB-Pascual Parrilla), Murcia, Spain
[3]Institute of Pharmacology and Structural Biology, University of Toulouse, CNRS, Toulouse, France
[4]Department of Biochemistry and Molecular Biology B and Immunology, Faculty of Medicine, University of Murcia, Murcia, Spain
[5]These authors contributed equally
[6]Lead contact
*Correspondence: julischachter@gmail.com (J.S.), pablopel@um.es (P.P.)
https://doi.org/10.1016/j.celrep.2025.115233

SUMMARY

Pyroptosis is a lytic cell death triggered by the cleavage of gasdermin (GSDM) proteins and subsequent pore formation by the N-terminal domain oligomerization in the plasma membrane. GSDMD is cleaved by caspase-1/-4/-5/-11 upon inflammasome activation and mediates interleukin (IL)-1β and IL-18 release. GSDMD pores favor ninjurin 1 (NINJ1)-induced plasma membrane rupture and cell death. Here, we demonstrate that GSDMD mediates early ATP release upon NLRP3 inflammasome activation independently of NINJ1, occurring before IL-1β release and cell death and constituting an early danger signal. The release of ATP is a transient signal terminated before the cells continue to permeabilize and die. The different N termini of GSDMA to -E are also able to release ATP and induce monocyte migration toward pyroptotic cells. This study reveals ATP release as an early and transient danger signal depending on GSDMD plasma membrane permeabilization, independently of the late stages of lytic cell death.

INTRODUCTION

Extracellular adenosine triphosphate (eATP) engages purinergic receptors and participates in various physiological processes, such as neurotransmission, cell death, vasodilatation, or cell differentiation.[1] eATP is also widely recognized as a danger signal, modulating several steps of the immune response: inflammation, chemotaxis, antigen presentation, modulation of T cell function, or macrophage activity.[2–4] Several stimuli, such as hypoxia, shear stress, swelling, or the presence of pathogens, can trigger ATP release through channels, pores, and exocytosis.[5–7] Ecto-nucleotidases terminate the action of eATP on specific purinergic receptors and generate new ligands for other purinergic receptors.[8,9]

Inflammation can be initiated by engaging the purinergic receptor P2X subunit 7 (P2X7R), which responds to mM concentrations of eATP. P2X7R mediates the efflux of intracellular K^+, leading to the activation of the nucleotide-binding domain and leucine-rich repeat-containing receptor with a pyrin domain 3 (NLRP3) inflammasome.[10,11] In turn, the NLRP3 inflammasome leads to caspase-1 activation and the cleavage of different cellular proteins, including pro-interleukin (IL)-1β and pro-IL-18, as well as gasdermin D (GSDMD).[12] The resulting GSDMD N-terminal (NT) fragment oligomerizes in the plasma membrane, forming pores and releasing IL-1β and IL-18.[13,14] GSDMD pores favor the oligomerization of the protein ninjurin 1 (NINJ1), inducing large ruptures in the membrane, leading to the lytic cell death termed pyroptosis.[15–17] Pyroptosis is a pro-inflammatory form of cell death characterized by cell swelling, membrane rupture, and the release of intracellular content, including different intracellular proteins, cytokines, inflammasome oligomers, and mitochondrial DNA.[18–20]

While the effects of eATP on NLRP3 inflammasome activation are well documented, the inflammatory signals promoting ATP release are less known. In this study, we found that, following NLRP3 inflammasome activation, ATP is released from macrophages as an early and transient danger signal, causing a non-linear accumulation of eATP dynamically controlled by ecto-nucleotidases. We demonstrate that ATP release is a regulated process requiring GSDMD membrane permeabilization and precedes IL-1β release and pyroptotic lytic cell death, showing that the late phases of NINJ1-mediated pyroptotic lytic cell death occur without ATP release. The NT fragments of GSDMA, -B, -C, -D, and -E were all also able to induce ATP release, with the accumulated eATP inducing monocyte migration.

RESULTS

NLRP3 inflammasome activation induces ATP release by GSDMD

Activation of the NLRP3 inflammasome by nigericin in lipopolysaccharide (LPS)-primed bone-marrow-derived macrophages (BMDMs) triggered a dose-dependent ATP release, causing a time-dependent increase of eATP concentration, followed by rapid degradation (Figure 1A). A similar eATP kinetic profile was observed in macrophages from P2X7R-deficient mice (Figures 1B and 1F). ATP release was inhibited by the specific NLRP3 inhibitor MCC950 (Figures 1A and 1B) and was not observed in resting, unprimed macrophages (Figure 1C), demonstrating the dependency of NLRP3. Furthermore, we found that ATP release was absent when NLRP3 was induced in *Casp1/11*$^{-/-}$ BMDMs (Figure 1D). Human macrophages derived from blood monocytes (Figure 1E), as well as THP-1, release ATP, but not *CASP1*$^{-/-}$ THP-1 cells (Figure 1F), after NLRP3 activation. We confirmed that human macrophages were able to release ATP dependent on NLRP3 and caspase-1.

BMDMs from mice deficient in GSDMD failed to accumulate eATP after NLRP3 inflammasome activation (Figure 1G). Since lytic cell death during pyroptosis downstream of GSDMD plasma membrane permeabilization is driven by NINJ1, we measured eATP release after NLRP3 activation in the presence of glycine, which inhibits NINJ1 clustering and avoids plasma membrane rupture.[13,21,22] We found that glycine did not affect ATP (Figures 1F and 1H) or IL-1β release after NLRP3 activation (Figure S1A) but did block lactate dehydrogenase (LDH) release. Furthermore, immortalized *Ninj1*$^{-/-}$ BMDMs, treated with LPS and nigericin, exhibited ATP release, while, as expected, immortalized *Gsdmd*$^{-/-}$ BMDMs did not (Figure 1I). Accordingly, immortalized *Ninj1*$^{-/-}$ BMDMs, as well as *Gsdmd*$^{-/-}$ BMDMs, released very low amounts of LDH compared with wild-type (WT) macrophages in response to the same treatment (Figures S1B–S1D). This demonstrates that GSDMD, but not NINJ1, is involved in ATP release during pyroptosis.

During treatments that induced ATP release, an early phase of eATP decrease was observed, though it was not included in the analysis. This decrease, likely due to mechanical stimulation, was independent of NLRP3 activation and pyroptosis, as it was unaffected by MCC950 and not observed in *Gsdmd*$^{-/-}$ macrophages (Figures 1A–1C and 1G–1I).

Although pannexin-1 and connexin-43 are reported to mediate ATP release in macrophages,[23] carbenoxolone (CBX) and gadolinium (Gd^{3+}), two generic inhibitors of these and other ATP conduits, did not affect eATP kinetics (Figures S2A and S2B). Overall, these results show that ATP release in macrophages is triggered soon after the activation of the NLRP3 inflammasome, following a process requiring caspase-1 activity and the presence of GSDMD. This process is not linked to the late phases of pyroptosis mediated by NINJ1 plasma membrane lysis.

eATP is hydrolyzed on the surface of macrophages during early pyroptosis

In the extracellular milieu, eATP can be hydrolyzed to eADP and inorganic phosphate by ecto-nucleotidases. To evaluate the ecto-ATPase activity present on the surface of LPS-primed macrophages after treatment with nigericin, we added increased concentrations of exogenous ATP to the assay medium, with these concentrations falling within the same range as the endogenous eATP concentrations shown in Figure 1.

ATP addition led to an immediate increase in eATP to a maximum, which allowed us to determine the subsequent eATP decrease kinetics (Figure S3A). The initial lineal decay in eATP was used to estimate ecto-ATPase activity at each ATP concentration (Figure S3B). The ecto-ATPase activity of the macrophages followed a linear function with ATP concentration, with the slope of the curve (K_{ATP}) amounting to 3.2 μM eATP/μM eATP (min·mg of protein) (Figure S3B). As compared to ecto-ATPase activity of other cell types,[24] BMDMs presented a relatively high eATP hydrolysis rate. Thus, the observed fast eATP degradation during pyroptosis is expected to play a regulatory role, preventing excessive and continuous ATP signaling.

ATP release dependent on NLRP3 activation precedes lytic cell death

To gain further insights into the relation of ATP release and cell death, we studied the kinetics of YO-PRO-1 (629 Da) uptake in LPS-primed BMDMs treated with nigericin. The average behavior of BMDMs shows that YO-PRO-1 uptake displays a sigmoidal internalization kinetics, with an initial lag phase of basal fluorescence followed by a rapid increase in dye uptake. Such a response was completely absent in *Gsdmd*$^{-/-}$ macrophages or in cells treated with MCC950 (Figure 2A). An analysis of individual cells shows that, following a lag phase, the sigmoidal phenomenon was sufficiently steep to be described as a near "all-or-none" uptake process (Figure 2B).

A frequency histogram of YO-PRO-1-positive cells was built, normalizing the initial time point (t = 0) to the moment the first cell in each experiment became YO-PRO positive. This analysis revealed that the majority of the macrophages (80.4%) exhibited a burst of dye uptake between 0 and 20 min (Figure 2C), with a peak at 14 min. The average time until the first cell became permeabilized was 23.3 ± 0.5 min, and after 30 min, macrophages that did not capture YO-PRO-1 remained unpermeabilized through the recording time. BMDMs from P2X7R-deficient mice showed a histogram shifted to the right, with a peak at 18 min and an average time to the first cell's permeabilization of 31.1 ± 0.5 min (Figure 2D). Moreover, the percentages of permeabilized cells differed significantly, with 85.5% of YO-PRO-1 positive in WT cells compared to 53.7% in *P2x7*$^{-/-}$ cells, suggesting a potential function of P2X7R in GSDMD pore formation. As P2X7R is not required for ATP release after NLRP3 activation, the observed delay in YO-PRO-1 uptake in P2X7R-deficient cells could indicate that the released ATP may stimulate YO-PRO-1 uptake in neighboring cells.

IL-1β and LDH release after NLRP3 activation exhibited non-linear release kinetics upon nigericin stimulation. However, the increase in IL-1β release was significantly faster and greater in relative magnitude compared to LDH (Figure 2E), suggesting two qualitatively different processes.

Glycine did not affect YO-PRO-1 uptake (Figure 2F), indicating that it measured GSDMD plasma membrane permeabilization. Therefore, YO-PRO-1 uptake and IL-1β release seem be

CellPress
OPEN ACCESS

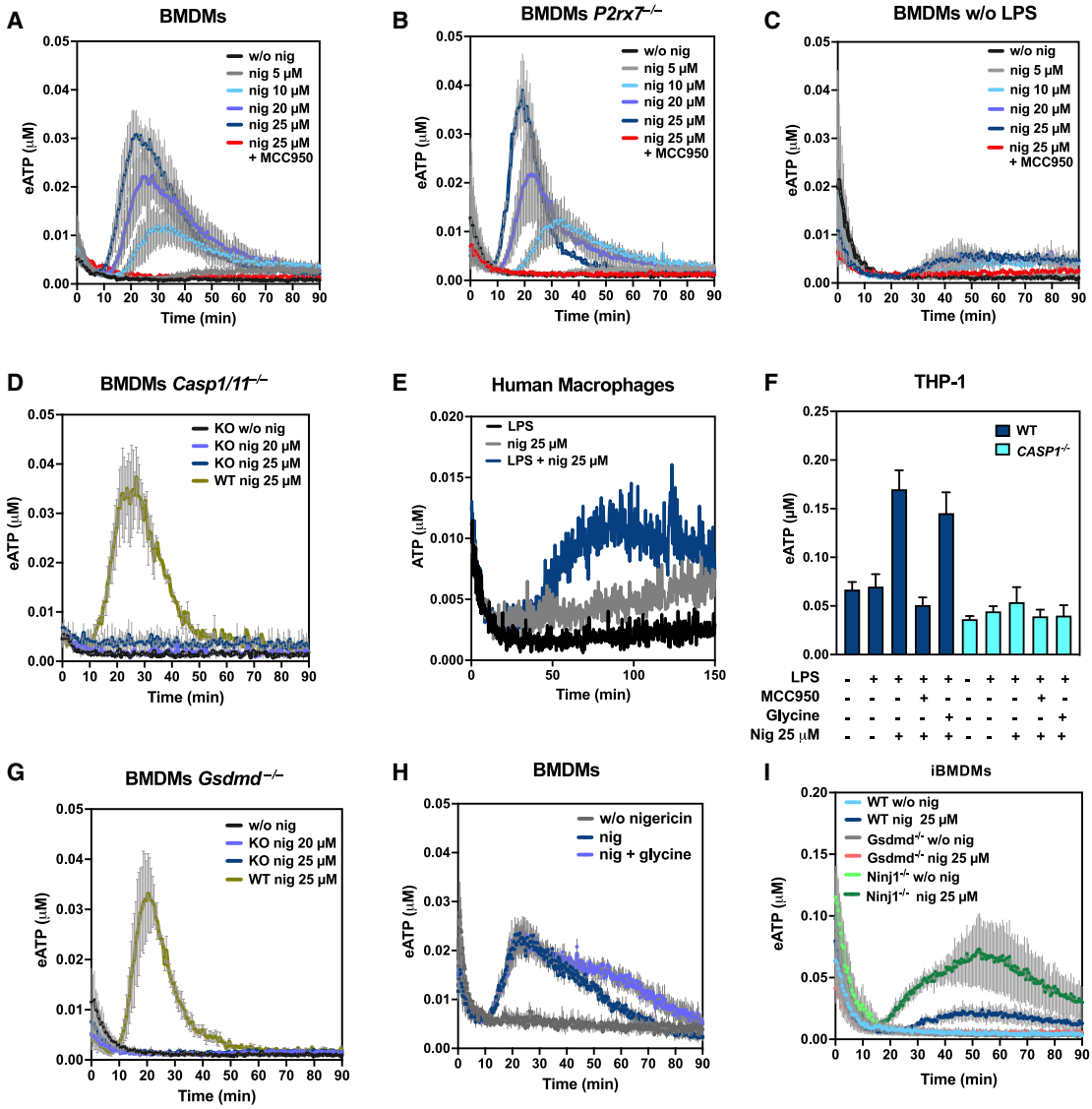

Figure 1. ATP release after NLRP3 activation is GSDMD dependent

(A–E) Kinetics of extracellular ATP (eATP) after canonical NLRP3 inflammasome activation in LPS-primed mouse bone-marrow-derived macrophages (BMDMs) (A, B, and D) or unprimed BMDMs (without [w/o] LPS) (C) obtained from wild-type (WT) (A and C), *P2rx7*$^{-/-}$ (B), or *Casp1/11*$^{-/-}$ (D) mice. The different curves show the eATP concentrations of macrophages treated with saline vehicle solution (black lines, w/o nigericin [nig]) or 5 μM nig (gray lines), 10 μM nig (light blue lines), 20 μM nig (blue lines), 25 μM nig (dark blue lines), or 25 μM nig with 10 μM MCC950 (red lines). To compare results using BMDMs from WT mice vs. the knockout (KO) genotype, the green lines in (D) represent eATP kinetics of BMDMs WT treated with 25 μM nig. Data are expressed in eATP concentration (μM) as the mean ± SEM of independent experiments (*N*) performed in duplicate (*n*), with $N = 3$ and $n = 2$ for cells from WT mice and $N = 2$ and $n = 2$ for cells from *P2rx7*$^{-/-}$ and *Casp1/11*$^{-/-}$ mice.

(E) Kinetics of eATP from LPS-primed human monocyte-derived macrophages treated with saline solution (black line) or 25 μM nig (blue line) or unprimed macrophages treated with 25 μM nig (gray line). Representative experiment of three experiments performed in duplicate is shown.

(F) THP-1 WT cells (dark blue bars) and THP-1 *CASP1*$^{-/-}$ (light blue bars) cells were primed or not with LPS and treated or not with 25 μM nig, 10 μM MCC950, or 5 mM glycine, as indicated in the bar graph. Data are expressed in eATP concentration (μM) at 120 min as the mean ± SEM of $N = 3$ and $n = 2$.

(G) Kinetics of eATP of BMDMs from WT (green line) or *Gsdmd*$^{-/-}$ (black, light blue, and blue lines) mice treated as in (A). Data are expressed in eATP concentration (μM) as the mean ± SEM of $N = 3$ and $n = 2$.

(H) LPS-primed BMDMs were treated with saline vehicle solution (gray line), 25 μM nig (blue line), or 25 μM nig with 5 mM glycine (light blue line). Data are expressed in eATP concentration (μM) as the mean ± SEM of $N = 3$ and $n = 2$.

(I) LPS-primed immortalized WT, *Gsdmd*$^{-/-}$, or *Ninj1*$^{-/-}$ BMDMs treated with saline solution (light blue for WT, gray for *Gsdmd*$^{-/-}$, and light green for *Ninj1*$^{-/-}$) or 25 μM nig (dark blue for WT, red for *Gsdmd*$^{-/-}$, and dark green for *Ninj1*$^{-/-}$). Data are expressed in eATP concentration (μM) as the mean ± SEM of $N = 3$ and $n = 2$. See also Figures S1–S3.

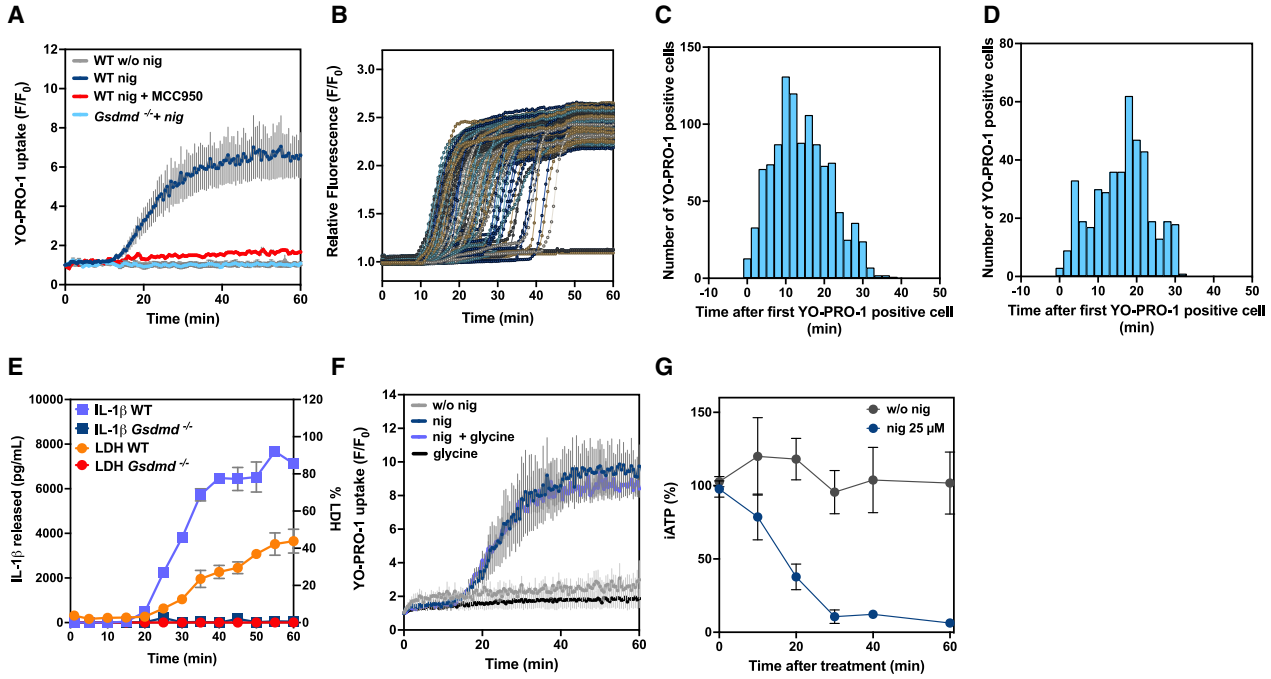

Figure 2. ATP release precedes pyroptotic lytic cell death

(A) YO-PRO-1 uptake from LPS-primed BDMDs from WT mice treated with nigericin (nig; dark blue line) or nig with 10 μM MCC950 (red line), unprimed cells treated with nig (gray line), or LPS-primed BMDMs from *Gsdmd*$^{-/-}$ mice treated with nig (light blue line). Data are the mean ± SEM of independent experiments (*N*) performed in duplicate (*n*), *N* = 3 and *n* = 2, and the fluorescence was normalized to the initial florescence in each experiment (F/F_0).

(B) YO-PRO-1 uptake of individual LPS-primed BMDMs treated with 25 μM nig at time = 0 (each macrophage is represented as a line). Representative experiment of 5 independent experiments is shown.

(C and D) Histogram showing the number of YO-PRO-1-positive cells obtained from LPS-primed BMDMs from wild-type (WT) (C) or *P2rx7*$^{-/-}$ (D) mice at different times of nig application. Each experiment was normalized by setting the time of the first YO-PRO-positive cell as time 0. Total numbers of cells = 1,098 (WT) and 432 (*P2rx7*$^{-/-}$), obtained from 5 (WT) or 3 (*P2rx7*$^{-/-}$) independent experiments, with ∼200 cells quantified in each experiment.

(E) Kinetics of IL-1β and LDH release from LPS-primed BDMDs treated with 20 μM nig. Light blue and orange lines are from WT mice and red and blue lines are from *Gsdmd*$^{-/-}$ mice. Results are the mean ± SEM for *N* = 3 and *n* = 2.

(F) YO-PRO-1 uptake from LPS-primed BDMDs treated with saline solution (gray line), 5 mM glycine (black line), 25 μM nig (dark blue line), or 25 μM nig and 5 mM glycine (light blue line). Results are the mean ± SEM for *N* = 3 and *n* = 2.

(G) Kinetic of intracellular ATP concentrations after canonical NLRP3 inflammasome activation in LPS-primed BMDMs treated with 25 μM nig (blue symbols) or not (gray symbols). Results are expressed as the percentage of total intracellular ATP and are the mean ± SEM for *N* = 3 independent experiments.

coincident in time and dependent on GSDMD, LDH release is right shifted and dependent on NINJ1, and ATP release is the earliest event dependent on the initial GSDMD permeabilization. The fact that YO-PRO-1 uptake appears after ATP release could mean that ATP diffusion through the initial GSDMD pores will be easy or could impair the influx of YO-PRO-1 or that YO-PRO-1 uptake does not effectively label early or transient GSDMD pores, as transient GSDMD pores are ∼10% the magnitude of a permeabilized cell.[25]

When NINJ1-dependent LDH release is initiated, most cells are already GSDMD permeabilized, and the eATP concentration starts to decrease to levels similar to the resting state. This suggests a novel concept, i.e., that the phase of plasma membrane rupture during pyroptosis may not be the primary moment for significant ATP release. In fact, besides the effect of ecto-nucleotidases removing eATP, the intracellular ATP levels also decline over time following NLRP3 activation, dropping to less than 2% after 30 min (Figure 2G). This ensures that even when large portions of the plasma membrane are damaged by NINJ1, ATP is no longer being released from cells. Thus, given the observed GSDMD dependence of ATP release without the participation of hemichannels and the fact that activated GSDMD forms large pores high enough to transport ATP but not LDH, it is tempting to speculate that GSDMD acts as an ATP conduit, allowing ATP release before plasma membrane rupture. By the time LDH is released, depending on NINJ1, intracellular ATP concentrations have dropped so low that there is insufficient chemical transmembrane gradient to drive further ATP release.

ATP is released through different GSDMs

To corroborate the role of GSDMD pore formation in ATP release, we studied the kinetics of ATP release in a recombinant system of HEK293T cells expressing either full-length GSDMD or the GSDMD NT domain. Discrete ATP concentrations were measured in the culture medium at different time points post-transfection. Cells transfected with the GSDMD NTs showed increased eATP levels at all time points, peaking at 6 h (Figure 3A). LDH release presented a gradual increase, reaching a

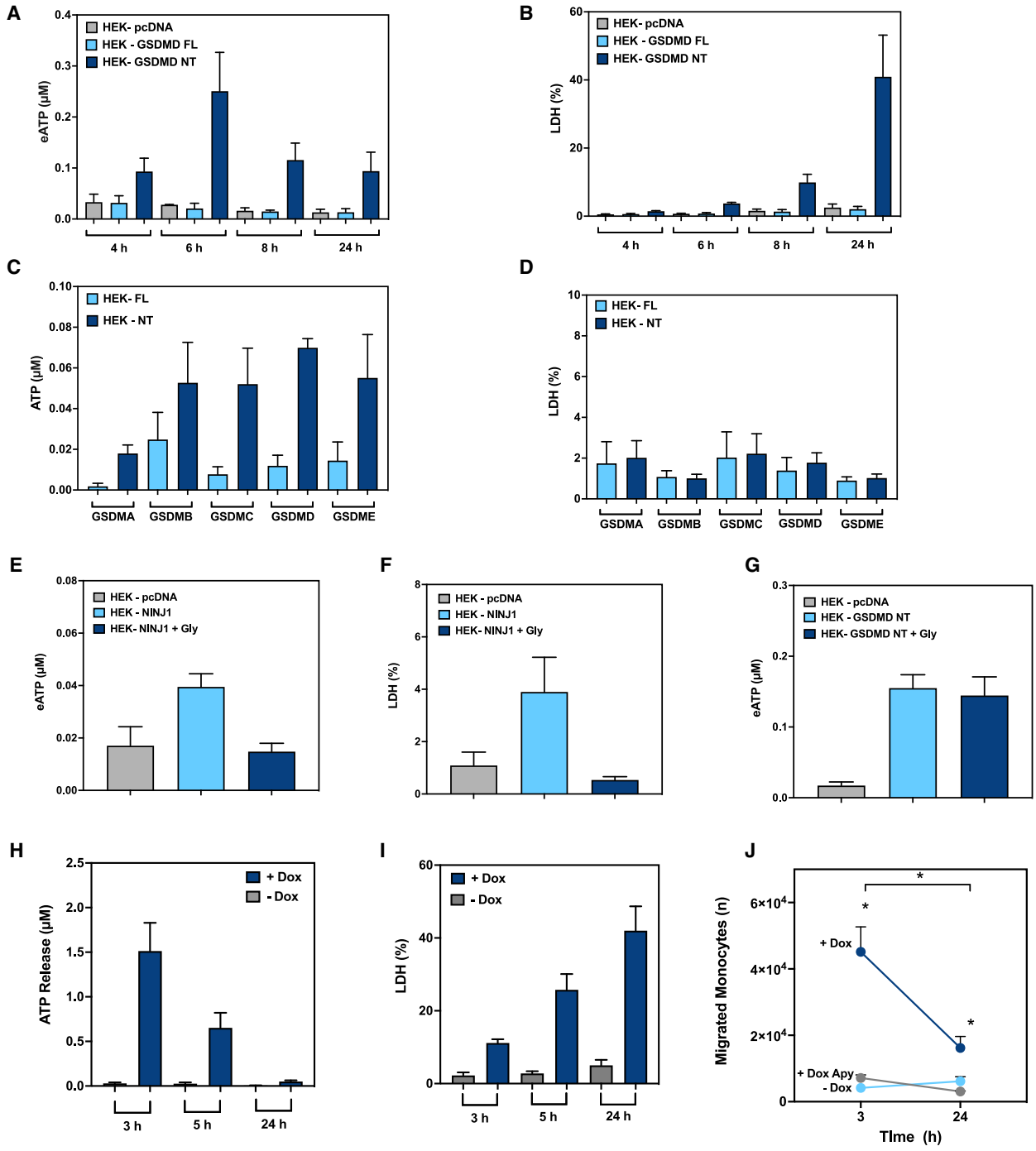

Figure 3. ATP is released from different GSDMs and NINJ1 and promotes cell migration

(A and B) Extracellular ATP (eATP) (A) and LDH (B) from HEK293T cells transfected with GSDMD full-length (FL), GSDMD N-terminal (NT), or pcDNA3.1 at 4, 6, 8, and 24 h after transfection. Results are the mean ± SEM of independent experiments (*N*), performed in duplicate (*n*), $N = 4$ and $n = 2$.

(C and D) eATP (C) and LDH (D) from HEK293T cells transfected with GSDMA, -B, -C, -D, and -E FL and NT at 4 h after transfection. Results are the mean ± SEM of $N = 3$ and $n = 2$.

(E and F) eATP (E) and LDH (F) from HEK293T cells transfected with pcDNA3.1 (control, gray bars), NINJ1 (light blue bars), or NINJ1 with 5 mM glycine (Gly) (dark blue bars) at 6 h after transfection. Results are the mean ± SEM of $N = 4$ and $n = 2$.

(G) eATP from HEK293T cells transfected with pcDNA3.1 (control, gray bars), GSDMD NT (light blue bars), or GSDMD NT with 5 mM Gly (dark blue bars) at 8 h after transfection. Results are the mean ± SEM of $N = 3$ and $n = 2$.

(legend continued on next page)

maximum at 24 h, the final time point measured (Figure 3B). Notably, at 4 h post-transfection, there was a significant release of ATP and less than 2% of LDH release.

Similarly, 4 h after transfection, the expression of the different NT fragments of GSDMA, -B, -C, and -E resulted in significant ATP release compared to their full-length counterparts (Figure 3C). At this time point, all GSDM NT fragments released less than 2% of LDH (Figure 3D), showing that ATP can permeate through the various GSDM pores before the onset of lytic cell death. As a control, we confirmed that after 24 h of transfection, all GSDM NT fragments were able to induce lytic cell death, as evidenced by a significant increase of LDH release (Figure S4).

Transfection of HEK293T cells with a plasmid encoding NINJ1 also led to an increase in both eATP concentration and LDH levels, which could be inhibited by glycine (Figures 3E and 3F). This suggests that early cell lysis induced by NINJ1 overexpression, in the absence of GSDM membrane permeabilization, also triggers ATP release. In contrast, GSDMD NT-induced ATP release was independent of NINJ1, as glycine had no effect on this process (Figure 3G). These findings collectively indicate that although ATP is capable of being released through NINJ1 plasma membrane rupture, as well as through GSDM pores, the exit of ATP during NLRP3-induced pyroptosis is restricted to GSDMD pores and does not occur during the later phases of NINJ1-induced plasma membrane rupture.

GSDMD-induced ATP release promotes monocyte migration

We finally investigated possible roles of GSDMD-dependent ATP release in immune cells using a recombinant doxycycline-induced system to control the formation of GSDMD pores. Using this system, we confirmed that ATP release initially increased after doxycycline addition and then decreased over time with doxycycline incubation, while LDH release progressively increased (Figures 3H and 3I).

We then used these supernatants to assess their effect on THP-1 monocyte migration. Supernatants collected after 3 and 24 h of doxycycline treatment both stimulated THP-1 migration, with a significantly greater number of monocytes migrating in response to the 3 h supernatants (Figures 3J and S5). Migration of THP-1 was inhibited when the supernatants were treated with apyrase (Figure 3J), indicating that nucleotides released during GSDMD-induced cell permeabilization were responsible for stimulating THP-1 migration.

To test the ability of released ATP to reach neighboring cells, we added HEK293T-GSDMD expressing a full-length or NT domain (2 h after transient transfection) to a monolayer of HEK293T cells stably expressing a chimeric plasma membrane luciferase (HEK293T-pmeLUC) in the presence of luciferin. The time-course response detected by HEK293T-pmeLUC cells showed that the HEK293T-GSDMD NT domain released significantly more ATP than the HEK293T-GSDMD full-length domain or mock-transfected HEK293T cells, and this ATP singling was prevented by treatment with apyrase (Figure S6A). The HEK293T-pmeLUC cells were calibrated with increasing concentrations of exogenous ATP (Figure S6B), and the slope obtained (Figure S6C) was used to calculate the concentration of ATP detected by HEK293T-pmeLUC in each condition (Figure S6A). The concentrations of ATP released by the HEK293T-GSDMD NT domain were in the mM range, showing that the paracrine extent of released ATP occurs at concentrations much higher than those detected in experiments in which ATP is measured in the entire supernatant.

Overall, our study highlights that ATP is released early during the initial permeabilization of the plasma membrane by GSDMD during NLRP3-induced pyroptosis, serving as an early and transient danger signal that induces monocyte migration before the onset of lytic cell death.

DISCUSSION

It is well established that eATP is a pro-inflammatory trigger that functions as a second signal for canonical NLRP3 inflammasome activation. In this report, we provide evidence that, in the early steps of inflammasome activation, ATP is released from macrophages in a GSDMD-dependent way. Our results suggest that upon NLRP3 inflammasome activation, ATP is transiently released and amplifies NLRP3 inflammasome effector responses by inducing monocyte migration.

Using 10^5 BMDMs per 50 μL assay, the maximum observed eATP concentration was approximately 30 nM. Although this *in vitro* concentration seems relatively low for activating most P2 receptors, the high abundance of BMDMs in the bone marrow suggests that micromolar eATP concentrations could be expected.

Moreover, low-micromolar eATP is compatible with purinergic signaling since eATP engages P2Y2 (EC_{50} ATP = 230 nM)[26] to enhance IL-1β release following NLRP3 activation.[27] In recombinant systems expressing the GSDMD NT fragment, eATP accumulates in micromolar levels.

Moreover, it has been described that cells can retain micromolar concentrations of eATP in their pericellular space without significant nucleotide convection into the bulk milieu.[28] The delay in YO-PRO-1 uptake and the reduced number of positive cells observed using P2X7R-deficient macrophages also pointed in this direction. These experiments showed that the ATP released after NLRP3 activation could be enough to activate P2X7R in the neighboring cells and also indicate that YO-PRO-1 uptake could happen by different pathways at the same time: GSDMD- and P2X7R-associated mechanisms. In this context, the HEK293T-pmeLUC system enabled the measurement of eATP in the immediate environment of the cell surface, where purinergic signaling occurs. Our experiments demonstrated that eATP released by the HEK293T-GSDMD NT was detected at high levels on the surface of HEK293T-pmeLUC.

(H and I) eATP (H) and LDH (I) from HEK293T cells with a doxycycline-inducible GSDMD NT expression system treated with doxycycline (blue bars) or not (gray bars) for 3, 5, or 24 h. Results are the mean ± SEM of $N = 3$ and $n = 2$.

(J) Migration of THP-1 cells through a transwell toward supernatants from inducible HEK293T cells treated as in (H) for 3 and 24 h with doxycycline (dark blue) or not (light blue). In gray, the supernatants of doxycycline were treated with apyrase. Results are the mean +SEM for $N = 3$ and $n = 2$. $^*p < 0.05$.

See also Figures S4–S6.

The relatively high eATP hydrolysis rate observed should also produce high concentrations of eADP, which in turn may activate P2Y1, P2Y12, and P2Y13 receptors[29] and potentially trigger cellular responses with inflammatory relevancy. For example, the activation of the P2Y12 receptor induces chemotaxis and chemokine release in tumor-associated macrophages.[30] In line, we found that extracellular nucleotides from cells expressing GSDMD pores were able to induce the migration of THP-1, suggesting the attraction of cells toward pyroptotic cells. Although P2Y1 and P2Y13 ADP receptors were identified in macrophages,[31] their role in the NLRP3 inflammasome or inflammation has not been characterized.

In addition to eADP accumulation caused by eATP hydrolysis, macrophages express ecto-nucleotidases NTPDase 1[32] and 5′ NT.[31] The coupled action of both enzymes may produce adenosine from eATP, with consequent activation of P1 receptors. It is well known that the activation of P1 receptors by adenosine contributes to regulating inflammation.[33]

Therefore, the eATP kinetics after NLRP3 activation initiate an early pro-inflammatory phase characterized by the accumulation of eATP and its hydrolysis product, eADP. This is followed by a later phase where adenosine exerts anti-inflammatory effects, probably contributing to the fine-tuning of inflammation.

Our results using glycine, a cytoprotective amino acid that inhibits NINJ1 oligomerization and subsequent plasma membrane rupture, along with studies in *Ninj1*-deficient macrophages, showed that ATP is released via a non-lytic mechanism prior to pyroptotic cell death, as evidenced by ATP efflux occurring before LDH release. Notably, YO-PRO-1 uptake was not inhibited by glycine, indicating that this fluorescent molecule can pass through GSDMD pores before the final lytic phase of pyroptotic cell death. As already reported,[16,22] the sole ectopic expression of NINJ1 in cells induces lytic cell death independently of GSDM pores. Here, we further discovered that under these conditions, NINJ1 oligomerization drives ATP release.

Our experiments showed that IL-1β and LDH release are distinct events. This aligns with previous studies showing that GSDMD pore formation triggers IL-1β (17 kDa) release independently of cell death.[13,19,34] In a subsequent phase of pyroptosis, GSDMD pores promote NINJ1-mediated cell membrane rupture, leading to the release of LDH (a 140 kDa tetrameric complex), which is too large to pass through GSDMD pores.[13,35]

However, the mechanism by which GSDMD pores induce NINJ1 oligomerization and plasma membrane rupture remains unclear. Our findings, consistent with other studies, demonstrated that blocking NINJ1 oligomerization at the plasma membrane impaired LDH release without affecting IL-1β release.[19,22,36]

Noteworthy, eATP kinetics revealed a transient increase of eATP concentrations before the onset of lytic pyroptotic cell death, with no differences observed when NINJ1 was inhibited or genetically inactivated. This suggests that ATP release during pyroptosis is a controlled process.

Moreover, we observed that intracellular concentrations of ATP dropped dramatically to less than 10% of their initial levels within 30 min of nigericin addition. LDH release begun around 25–30 min under our conditions, suggesting that cells begin their path to silent death soon after NLRP3 activation.

On the other hand, ATP and IL-1β release occur earlier than the lytic phase of pyroptotic cell death, suggesting that ATP release could be a general danger signal resulting from initial small GSDMD pores, which may be too small to allow for IL-1β release.[37,38] Our study further indicates that ATP release serves as a broad inflammatory danger signal, released through various GSDM pores even in cells that do not express IL-1β, impacting both immune and non-immune cells. These findings indicate that ATP release through GSDMD pores is an early and transient non-lytic event occurring after canonical NLRP3 inflammasome activation and before NINJ1-dependent cell lysis.

Limitations of the study

While our study provides significant insights into the early release of ATP mediated by GSDMD in BMDMs, the precise structural basis of ATP transport through GSDMD pores remains unresolved. While much progress has been made in understanding the molecular mechanisms regulating GSDMD pore formation, how these regulatory mechanisms are coordinated in time and space, particularly in the context of ATP transmembrane permeability, remains to be further explored. Our analysis primarily focused on eATP as a danger signal, but other molecules (like, e.g., other nucleotides) potentially released through GSDMD pores and their biological relevance were not investigated.

RESOURCE AVAILABILITY

Lead contact

Further information and requests for resources and reagents should be directed to and will be fulfilled by the lead contact, Dr. Pablo Pelegrin (pablopel@um.es).

Materials availability

Plasmids and cells developed in the present study are available upon request to the lead contact, Dr. Pablo Pelegrin (pablopel@um.es).

Data and code availability

- All data reported in this paper will be shared by the lead contact upon request.
- This paper does not report original code.
- Any additional information required to reanalyze the data reported in this paper is available from the lead contact upon request.

ACKNOWLEDGMENTS

We thank I. Couillin (CNRS Orleans, France) for *Gsdmd*$^{-/-}$ mice, I. Hafner (National Institute of Chemistry, Ljubljana, Slovenia) for *Gsdmd*$^{-/-}$ and *Ninj1*$^{-/-}$ iBMDMs, F. Di Virgilio (University of Ferrara, Italy) for pmeLuc cells, C. Martínez (IMIB, Murcia, Spain) for buffy coats, M.C. Baños and A.I. Gomez (IMIB, Murcia, Spain) for technical assistance with molecular and cellular biology, and the members of Pelegrin's laboratory for comments and suggestions thought the development of this project. This work was supported by grants from MCIN/AEI/10.13039/501100011033, FEDER/Ministerio de Ciencia, Innovación y Universidades – Agencia Estatal de Investigación (grants PID2020-116709RB-I00 and RED2022-134511-T to P.P.), MCIN/AEI/10.13039/501100011033 and European Union «Next Generation EU/PRTR» (grant CNS2022-135105 to P.P.), Fundación Séneca (grant 21897/PI/22 to P.P.), the Instituto de Salud Carlos III (grants DTS21/00080 and AC22/00009 to P.P.), the EU Horizon 2020 project PlasticHeal (grant 965196 to P.P.), and an Invivogen-ANRT CIFRE PhD grant (Invivogen) to M.P. and E.M. L.H.-N. was supported by fellowship 21214/FPI/19 (Fundación Séneca, Spain) and AG fellowship PRE2021-100356 (Ministerio de Economía y Competitividad). J.S. was supported by Universidad de Murcia (R-745/2022) and Fundación Séneca (22192/IV/23). J.S. and P.J.S. are

career researchers of Consejo Nacional de Investigaciones Científicas y Técnicas.

AUTHOR CONTRIBUTIONS

Conceptualization, validation, methodology, data curation, and writing – original draft, P.P. and J.S.; formal analysis, P.P., J.S., P.J.S., A.G., D.A.-B., L.H.-N., and M.P.; investigation, A.G., J.S., D.A.-B., and L.H.-N.; resources, M.P. A.B.P.-O., and E.M.; writing – review & editing, P.P., J.S., and P.J.S.; supervision and project administration, P.P.; funding acquisition, P.P. and J.S.

DECLARATION OF INTERESTS

P.P. declares that he is an inventor on a patent (PCT/EP2020/056729) and a consultant of Viva *In Vitro* Diagnostics SL. P.P., L.H.-N., and D.A.-B. are co-founders of Viva *In Vitro* Diagnostics SL but declare that the research was conducted in the absence of any commercial or financial relationships that could be construed as a potential conflict of interest.

STAR★METHODS

Detailed methods are provided in the online version of this paper and include the following:

- KEY RESOURCES TABLE
- EXPERIMENTAL MODEL AND STUDY PARTICIPANT DETAILS
  - Animals
  - Human samples
  - Immortalized macrophages
  - Cell lines
  - Generation of HEK-293T with an inducible GSDMD NT system
- METHOD DETAILS
  - ATP measurements
  - YO-PRO-1 uptake assay
  - ELISA
  - Lactate dehydrogenase (LDH) assay
  - Monocyte migration assay
- QUANTIFICATION AND STATISTICAL ANALYSIS
  - Statistical methods

SUPPLEMENTAL INFORMATION

Supplemental information can be found online at https://doi.org/10.1016/j.celrep.2025.115233.

Received: November 9, 2023
Revised: October 25, 2024
Accepted: January 3, 2025
Published: February 1, 2025

REFERENCES

1. Giuliani, A.L., Sarti, A.C., and Di Virgilio, F. (2019). Extracellular nucleotides and nucleosides as signalling molecules. Immunol. Lett. *205*, 16–24. https://doi.org/10.1016/J.IMLET.2018.11.006.
2. Cekic, C., and Linden, J. (2016). Purinergic regulation of the immune system. Nat. Rev. Immunol. *16*, 177–192. https://doi.org/10.1038/NRI.2016.4.
3. Kepp, O., Loos, F., Liu, P., and Kroemer, G. (2017). Extracellular nucleosides and nucleotides as immunomodulators. Immunol. Rev. *280*, 83–92. https://doi.org/10.1111/IMR.12571.
4. Kobayashi, D., Umemoto, E., and Miyasaka, M. (2023). The role of extracellular ATP in homeostatic immune cell migration. Curr. Opin. Pharmacol. *68*, 102331. https://doi.org/10.1016/J.COPH.2022.102331.
5. Fitz, J.G. (2007). Regulation of cellular ATP release. Trans. Am. Clin. Climatol. Assoc. *118*, 199–208.
6. Dosch, M., Gerber, J., Jebbawi, F., and Beldi, G. (2018). Mechanisms of ATP Release by Inflammatory Cells. Int. J. Mol. Sci. *19*, 1222. https://doi.org/10.3390/IJMS19041222.
7. Taruno, A. (2018). ATP Release Channels. Int. J. Mol. Sci. *19*, 808. https://doi.org/10.3390/IJMS19030808.
8. Zimmermann, H. (2021). Ectonucleoside triphosphate diphosphohydrolases and ecto-5'-nucleotidase in purinergic signaling: how the field developed and where we are now. Purinergic Signal. *17*, 117–125. https://doi.org/10.1007/S11302-020-09755-6.
9. Zimmermann, H. (2021). History of ectonucleotidases and their role in purinergic signaling. Biochem. Pharmacol. *187*, 114322. https://doi.org/10.1016/j.bcp.2020.114322.
10. Pelegrin, P. (2021). P2X7 receptor and the NLRP3 inflammasome: Partners in crime. Biochem. Pharmacol. *187*, 114385. https://doi.org/10.1016/J.BCP.2020.114385.
11. Tapia-Abellán, A., Angosto-Bazarra, D., Alarcón-Vila, C., Baños, M.C., Hafner-Bratkovič, I., Oliva, B., and Pelegrín, P. (2021). Sensing low intracellular potassium by NLRP3 results in a stable open structure that promotes inflammasome activation. Sci. Adv. *7*, eabf4468. https://doi.org/10.1126/SCIADV.ABF4468.
12. Liu, X., Zhang, Z., Ruan, J., Pan, Y., Magupalli, V.G., Wu, H., and Lieberman, J. (2016). Inflammasome-activated gasdermin D causes pyroptosis by forming membrane pores. Nature *535*, 153–158. https://doi.org/10.1038/NATURE18629.
13. Evavold, C.L., Ruan, J., Tan, Y., Xia, S., Wu, H., and Kagan, J.C. (2018). The Pore-Forming Protein Gasdermin D Regulates Interleukin-1 Secretion from Living Macrophages. Immunity *48*, 35–44.e6. https://doi.org/10.1016/J.IMMUNI.2017.11.013.
14. Heilig, R., Dick, M.S., Sborgi, L., Meunier, E., Hiller, S., and Broz, P. (2018). The Gasdermin-D pore acts as a conduit for IL-1β secretion in mice. Eur. J. Immunol. *48*, 584–592. https://doi.org/10.1002/EJI.201747404.
15. Kelley, N., Jeltema, D., Duan, Y., and He, Y. (2019). The NLRP3 Inflammasome: An Overview of Mechanisms of Activation and Regulation. Int. J. Mol. Sci. *20*, 3328. https://doi.org/10.3390/IJMS20133328.
16. Kayagaki, N., Kornfeld, O.S., Lee, B.L., Stowe, I.B., O'Rourke, K., Li, Q., Sandoval, W., Yan, D., Kang, J., Xu, M., et al. (2021). NINJ1 mediates plasma membrane rupture during lytic cell death. Nature *591*, 131–136. https://doi.org/10.1038/S41586-021-03218-7.
17. Degen, M., Santos, J.C., Pluhackova, K., Cebrero, G., Ramos, S., Jankevicius, G., Hartenian, E., Guillerm, U., Mari, S.A., Kohl, B., et al. (2023). Structural basis of NINJ1-mediated plasma membrane rupture in cell death. Nature *618*, 1065–1071. https://doi.org/10.1038/S41586-023-05991-Z.
18. Baroja-Mazo, A., Martín-Sánchez, F., Gomez, A.I., Martínez, C.M., Amores-Iniesta, J., Compan, V., Barberà-Cremades, M., Yagüe, J., Ruiz-Ortiz, E., Antón, J., et al. (2014). The NLRP3 inflammasome is released as a particulate danger signal that amplifies the inflammatory response. Nat. Immunol. *15*, 738–748. https://doi.org/10.1038/NI.2919.
19. de Torre-Minguela, C., Gómez, A.I., Couillin, I., and Pelegrín, P. (2021). Gasdermins mediate cellular release of mitochondrial DNA during pyroptosis and apoptosis. FASEB J. *35*, e21757. https://doi.org/10.1096/FJ.202100085R.
20. Phulphagar, K., Kühn, L.I., Ebner, S., Frauenstein, A., Swietlik, J.J., Rieckmann, J., and Meissner, F. (2021). Proteomics reveals distinct mechanisms regulating the release of cytokines and alarmins during pyroptosis. Cell Rep. *34*, 108826. https://doi.org/10.1016/J.CELREP.2021.108826.
21. Fink, S.L., and Cookson, B.T. (2006). Caspase-1-dependent pore formation during pyroptosis leads to osmotic lysis of infected host macrophages. J. Immunol. *8*, 1812–1825. https://doi.org/10.1111/J.1462-5822.2006.00751.X.
22. Borges, J.P., Sætra, R.S.R., Volchuk, A., Bugge, M., Devant, P., Sporsheim, B., Kilburn, B.R., Evavold, C.L., Kagan, J.C., Goldenberg, N.M., et al. (2022). Glycine inhibits NINJ1 membrane clustering to suppress

plasma membrane rupture in cell death. Elife *11*, e78609. https://doi.org/10.7554/ELIFE.78609.

23. Muñoz, M.F., Griffith, T.N., and Contreras, J.E. (2021). Mechanisms of ATP release in pain: role of pannexin and connexin channels. Purinergic Signal. *17*, 549–561. https://doi.org/10.1007/S11302-021-09822-6.
24. Schachter, J., Alvarez, C.L., Bazzi, Z., Faillace, M.P., Corradi, G., Hattab, C., Rinaldi, D.E., Gonzalez-Lebrero, R., Molineris, M.P., Sévigny, J., et al. (2021). Extracellular ATP hydrolysis in Caco-2 human intestinal cell line. Biochim. Biophys. Acta. Biomembr. *1863*, 183679. https://doi.org/10.1016/J.BBAMEM.2021.183679.
25. Rühl, S., Shkarina, K., Demarco, B., Heilig, R., Santos, J.C., and Broz, P. (2018). ESCRT-dependent membrane repair negatively regulates pyroptosis downstream of GSDMD activation. Science *362*, 956–960. https://doi.org/10.1126/SCIENCE.AAR7607.
26. Jacobson, K.A., Delicado, E.G., Gachet, C., Kennedy, C., von Kügelgen, I., Li, B., Miras-Portugal, M.T., Novak, I., Schöneberg, T., Perez-Sen, R., et al. (2020). Update of P2Y receptor pharmacology: IUPHAR Review 27. Br. J. Pharmacol. *177*, 2413–2433. https://doi.org/10.1111/BPH.15005.
27. de la Rosa, G., Gómez, A.I., Baños, M.C., and Pelegrín, P. (2020). Signaling Through Purinergic Receptor P2Y2 Enhances Macrophage IL-1β Production. Int. J. Mol. Sci. *21*, 4686. https://doi.org/10.3390/IJMS21134686.
28. Yegutkin, G.G., Mikhailov, A., Samburski, S.S., and Jalkanen, S. (2006). The Detection of Micromolar Pericellular ATP Pool on Lymphocyte Surface by Using Lymphoid Ecto-Adenylate Kinase as Intrinsic ATP Sensor. Mol. Biol. Cell *17*, 3378–3385. https://doi.org/10.1091/MBC.E05-10-0993.
29. von Kügelgen, I. (2021). Molecular pharmacology of P2Y receptor subtypes. Biochem. Pharmacol. *187*, 114361. https://doi.org/10.1016/J.BCP.2020.114361.
30. Kloss, L., Dollt, C., Schledzewski, K., Krewer, A., Melchers, S., Manta, C., Sticht, C., Torre, C.d.l., Utikal, J., Umansky, V., and Schmieder, A. (2019). ADP secreted by dying melanoma cells mediates chemotaxis and chemokine secretion of macrophages via the purinergic receptor P2Y12. Cell Death Dis. *10*, 760. https://doi.org/10.1038/S41419-019-2010-6.
31. Merz, J., Nettesheim, A., von Garlen, S., Albrecht, P., Saller, B.S., Engelmann, J., Hertle, L., Schäfer, I., Dimanski, D., König, S., et al. (2021). Pro- and anti-inflammatory macrophages express a sub-type specific purinergic receptor profile. Purinergic Signal. *17*, 481–492. https://doi.org/10.1007/S11302-021-09798-3.
32. Lévesque, S.A., Kukulski, F., Enjyoji, K., Robson, S.C., and Sévigny, J. (2010). NTPDase1 governs P2X7-dependent functions in murine macrophages. Eur. J. Immunol. *40*, 1473–1485. https://doi.org/10.1002/EJI.200939741.
33. Antonioli, L., Fornai, M., Blandizzi, C., Pacher, P., and Haskó, G. (2019). Adenosine signaling and the immune system: When a lot could be too much. Immunol. Lett. *205*, 9–15. https://doi.org/10.1016/J.IMLET.2018.04.006.
34. Xia, S., Zhang, Z., Magupalli, V.G., Pablo, J.L., Dong, Y., Vora, S.M., Wang, L., Fu, T.M., Jacobson, M.P., Greka, A., et al. (2021). Gasdermin D pore structure reveals preferential release of mature interleukin-1. Nature *593*, 607–611. https://doi.org/10.1038/S41586-021-03478-3.
35. Russo, H.M., Rathkey, J., Boyd-Tressler, A., Katsnelson, M.A., Abbott, D.W., and Dubyak, G.R. (2016). Active Caspase-1 Induces Plasma Membrane Pores That Precede Pyroptotic Lysis and Are Blocked by Lanthanides. J. Immunol. *197*, 1353–1367. https://doi.org/10.4049/JIMMUNOL.1600699.
36. Verhoef, P.A., Kertesy, S.B., Lundberg, K., Kahlenberg, J.M., and Dubyak, G.R. (2005). Inhibitory effects of chloride on the activation of caspase-1, IL-1beta secretion, and cytolysis by the P2X7 receptor. J. Immunol. *175*, 7623–7634. https://doi.org/10.4049/JIMMUNOL.175.11.7623.
37. Santa Cruz Garcia, A.B., Schnur, K.P., Malik, A.B., and Mo, G.C.H. (2022). Gasdermin D pores are dynamically regulated by local phosphoinositide circuitry. Nat. Commun. *13*, 52. https://doi.org/10.1038/S41467-021-27692-9.
38. Tsuchiya, K., Nakajima, S., Hosojima, S., Thi Nguyen, D., Hattori, T., Manh Le, T., Hori, O., Mahib, M.R., Yamaguchi, Y., Miura, M., et al. (2019). Caspase-1 initiates apoptosis in the absence of gasdermin D. Nat. Commun. *10*, 2091. https://doi.org/10.1038/S41467-019-09753-2.
39. Evavold, C.L., Hafner-Bratkovič, I., Devant, P., D'Andrea, J.M., Ngwa, E.M., Boršić, E., Doench, J.G., LaFleur, M.W., Sharpe, A.H., Thiagarajah, J.R., and Kagan, J.C. (2021). Control of gasdermin D oligomerization and pyroptosis by the Ragulator-Rag-mTORC1 pathway. Cell *184*, 4495–4511.e19. https://doi.org/10.1016/j.cell.2021.06.028.
40. Devant, P., Boršić, E., Ngwa, E.M., Xiao, H., Chouchani, E.T., Thiagarajah, J.R., Hafner-Bratkovič, I., Evavold, C.L., and Kagan, J.C. (2023). Gasdermin D pore-forming activity is redox-sensitive. Cell Rep. *42*, 112008. https://doi.org/10.1016/j.celrep.2023.112008.
41. Pellegatti, P., Falzoni, S., Pinton, P., Rizzuto, R., and Di Virgilio, F. (2005). A novel recombinant plasma membrane-targeted luciferase reveals a new pathway for ATP secretion. Mol. Biol. Cell *16*, 3659–3665. https://doi.org/10.1091/MBC.E05-03-0222.
42. Barbera-Cremades, M., Baroja-Mazo, A., Gomez, A.I., Machado, F., Di Virgilio, F., and Pelegrín, P. (2012). P2X7 receptor-stimulation causes fever via PGE2 and IL-1β release. FASEB J. *26*, 2951–2962. https://doi.org/10.1096/fj.12-205765.

STAR★METHODS

KEY RESOURCES TABLE

REAGENT or RESOURCE	SOURCE	IDENTIFIER
Biological samples		
Human macrophages	Monocyte-derived macrophages from healthy donors.	N/A
Chemicals, peptides, and recombinant proteins		
Lipopolysaccharides from Escherichia coli O55:B5	Sigma-Aldrich	L6529
Nigericin sodium salt	Sigma-Aldrich	N7143
MCC950 (CP-456773)	Sigma-Aldrich	5.38120
Adenosine 5′-triphosphate disodium salt hydrate (ATP)	Sigma-Aldrich	A2383
Triton X-100	Sigma-Aldrich	T9284
YO-PRO-1	Invitrogen	P3581
4-(2-Hydroxyethyl)piperazine-1-ethanesulfonic acid (HEPES)	Sigma-Aldrich	H3375
D-Glucose	PanReac AppliChem	131341
Potassium chloride (KCl)	PanReac AppliChem	141494
Calcium chloride ($CaCl_2$)	Sigma-Aldrich	C7902
Magnesium chloride ($MgCl_2$)	Sigma-Aldrich	M2670
Sodium chloride (NaCl)	Supelco	1.06404
Luciferase from Photinus pyralis	Sigma-Aldrich	L9420
Coenzyme A	Sigma-Aldrich	C3144
D-Luciferin	Invitrogen	L2912
Histopaque-1077	Sigma-Aldrich	10771
Digitonin	Sigma-Aldrich	D141
Percoll	Sigma-Aldrich	P1644
Critical commercial assays		
Mouse IL-1 beta/IL-1F2 Quantikine ELISA Kit	R&D Systems	MLB00C-1
SepMate falcon tubes	Stemcell	85415
LDH detection kit	Roche	Kit 11644793001
Experimental models: Cell lines		
iBMDMs	Produced by Dr I. Hafner (National Institute of Chemistry, Ljubljana, Slovenia) Evavold et al.[39] Devant et al.[40]	N/A
THP-1	American Type Culture Collection	TIB-202
HEK-293T	American Type Culture Collection	CRL-11268
HEK-293T pmeLuc	Pellegatti et al.[41]	N/A
Inducible HEK-293FT-GSDMD-NT	This study	N/A
Experimental models: Organisms/strains		
C57BL/6J	Jackson Laboratories	RRID:MGI:3028467
B6.129P2-P2rx7tm1Gab/J	Jackson Laboratories	RRID:MGI:J:66835
B6N.129S2-Casp1tm1Flv/J	Jackson Laboratories	RRID:MGI:J:24258
C57BL/6J $Gsdmd^{-/-}$ mice	Heilig et al.[14]	N/A
Recombinant DNA		
pcDNA3.1 GSDMD FL	This study	N/A
pcDNA3.1 GSDMD NT	This study	N/A
pcDNA3.1 GSDMA FL	This study	N/A
pcDNA3.1 GSDMA NT	This study	N/A
pcDNA3.1 GSDMB FL	This study	N/A

(*Continued on next page*)

Continued

REAGENT or RESOURCE	SOURCE	IDENTIFIER
pcDNA3.1 GSDMB NT	This study	N/A
pcDNA3.1 GSDMC FL	This study	N/A
pcDNA3.1 GSDMC NT	This study	N/A
pcDNA3.1 GSDME FL	This study	N/A
pcDNA3.1 GSDME NT	This study	N/A
pcDNA3.1 NINJ1	This study	N/A
Software and algorithms		
GraphPad Prism version	GraphPad Software	https://www.graphpad.com
FCS Express Software	*De Novo* Software	https://denovosoftware.com/
Other		
Penicillin-Streptomycin	Corning	30-002-CI
Dulbecco's modified Eagle's medium (DMEM-F12) w/o L-Glutamine, w/o HEPES Sterile Filtered	Biowest	L0090-500
L-Glutamine	Gibco	25030–032
Fetal Bovine Serum (FBS)	Biowest	S181A
Bovine Serum Albumin (BSA)	Sigma-Aldrich	A4503
OptiMEM reduced Serum Media	Gibco	51985–026
GlutaMAX	ThermoFisher	35050038
RPMI-1640	Sigma-Aldrich	R0883
Human Serum	Biowest	S181A
hGM-CFS	Biolegend	572903
Lipofectamine 2000	Invitrogen	11668–019
Phorbol 12-myristate 13-acetate (PMA)	Sigma-Aldrich	P8139
Doxycycline	Selleckchem	S5159
Apyrase	Sigma-Aldrich	A6410
Carbenoxolone disodium salt	Sigma-Aldrich	C4790
Gadolinium (III) chloride	Sigma-Aldrich	439770
Zeocin	Gibco	R25001
TrypLE Express	Gibco	12604–013
Inserts TC	Sarstedt	83.3932.500
BD Trucount Tubes	BD Biosciences	663028

EXPERIMENTAL MODEL AND STUDY PARTICIPANT DETAILS

Animals

C57BL/6 (wild type, WT) mice were purchased from Harlan. P2X7R-deficient mice (*P2rx7*$^{-/-}$) were purchased from Jackson (Solle et al., 2001), and *Gsdmd*$^{-/-}$, double caspase-1/11-deficient (*Casp1/11*$^{-/-}$) (Heilig et al., 2018, Kuida et al., 1995) were all on C57BL/6 background. For all experiments, both male and female mice between 8 and 10 weeks of age bred under SPF conditions were used in accordance with the University Hospital Virgen Arrixaca animal experimentation guidelines, and the Spanish national (RD 53/2013 and Law 6/2013) and EU (86/609/EEC and 2010/63/EU) legislation. According to legislation cited above, and local ethics committee from University of Murcia review approval (#738/2021), authorization is not needed, since mice were euthanized by CO_2 inhalation and used to obtain bone marrow; no procedure was undertaken which compromised animal welfare (chapter 1, article 3 of RD 53/2013).

Human samples

Bone marrow derived-macrophages (BMDMs) were obtained from wild type or knockout mice as described[42] and maintained in Dulbecco's modified Eagle's medium (DMEM-F12) supplemented with 10% FBS and 2 mM GlutaMax and 1% of penicilin-streptomycin.

Blood samples from male and female healthy humans volunteers included in this study, who gave written informed consent, were collected, and processed following standard operating procedures with appropriate approval of the Ethical Committee of the Clinical University Hospital Virgen de la Arrixaca (Murcia, Spain) with reference #2021-7-9-HCUVA. Human peripheral blood mononuclear cells (PBMCs) were isolated from whole blood samples using Ficoll-based gradient separation method. The blood samples were

added on the top chamber of a SepMate Falcon tube, containing 15 mL of Ficoll with 1.077 g/mL density. The tubes were centrifugated at 1.200 x g during 10 min and the PBMCs fraction was removed. The PMBCs were washed with PBS, suspended on OptiMEM, counted and 2 x 10^8 cell were added to 10 mL of Percoll. The tubes were centrifugated at 580 x g and the monocytes obtained were suspended in RPMI 1640 medium supplemented with 10% of human serum and seeded on 24-well plates at a density of 5x10^5 cells by well. After 3 days, the cells were washed and the differentiated macrophages were maintained 4 days until use.

Immortalized macrophages

Immortalized bone marrow-derived macrophages (iBMDMs) WT, *Gsdmd*$^{-/-}$ and *Ninj1*$^{-/-}$ were a gift from Dr. I. Hafner (National Institute of Chemistry, Ljubljana, Slovenia).[39,40] The iBMDMs were grown in DMEM-F12 supplemented with 10% FBS.

Cell lines

Cell lines used in this study were not authenticated, but were free of mycoplasma by routinely testing with the MycoProbe Mycoplasma Detection Kit following manufacturer instructions (R&D Systems).

THP-1 cells were maintained in RPMI 1640 media supplemented with 10% FBS and to measure ATP release, THP-1 were differentiated to macrophages with 0.5 μM PMA for 30 min before NLRP3 activation. For cell migration, THP-1 were not treated with PMA.

All types of macrophages were primed with LPS (1 μg/mL, 4h) and subsequent canonical NLRP3 inflammasome activation was achieved with nigericin at the indicated concentrations.

HEK-293T cells were maintained in DMEM-F12 supplemented with 10% FBS. For transfection with GSDMA, GSDMB, GSDMC, GSDMD, GSDME and NINJ1, cells were incubated at least 16 to allow adhesion to the plate before cationic lipid-based transfection using Lipofectamine 2000 (Invitrogen) according to the manufacturer's instruction. Briefly, two solutions of 50 μL of Opti-MEM containing a mix of 1–2 μg of total plasmid DNA (tube A) and 3 μL of Lipofectamine 2000 (tube B) were prepared and incubated 5 min at room temperature. After this period of time, the volume of DNA tube (A) was added into Lipofectamine 2000 tube (B), mixed gently and incubated 20 min at RT to allow lipid/DNA complexes formation and then added drop by drop to the cells. The plate was swirled gently and incubated at 37°C until the times indicated to extracellular ATP or LDH determinations.

HEK-293T stably transfected with plasma membrane luciferase (HEK-293T-pmeLUC)[41] were a gift of Prof. F. Di Virgilio (University of Ferrara, Italy). Cells were maintained in DMEM-F12 supplemented with 10% FBS and 1% of penicillin-streptomycin.

Generation of HEK-293T with an inducible GSDMD NT system

HEK293FT TREx-GSDMD-NT inducible system by doxycycline were generated by T-REx Complete Kit, with pcDNA4/TO Vector (K102001, ThermoFisher). The cells were maintained in DMEM-F12 supplemented with 20% FBS, 1% L-Glutamine, 1% of penicillin-streptomycin (Corning) and with 100 μg/ml zeocin (Gibco). Induction of GSDMD-NT was achieved by doxycycline treatment (10 ng/ml) for 3, 5 or 24 h.

METHOD DETAILS

ATP measurements

Extracellular ATP concentration in the supernatants were measured with the luciferase-luciferin assay (Strehler, 2006). BMDMs were plated in a 96-well plate and the culture media was replaced with basal salt solution containing 130 mM NaCl, 5 mM KCl, 1.5 mM $CaCl_2$, 1 mM $MgCl_2$, 25 mM Na-HEPES (adjusted to pH 7.5 at room temperature), 5 mM glucose, 0.1% BSA, 47.8 μM D-Luciferin, 0.5 μM luciferase and 0.1 mg/mL of CoA. For extracellular ATP calculations, a standard curve (from 10 to 200 nM ATP) was used. Bioluminescence measured were performed in a BioTek Synergy *Neo*2 Hybrid Multimode Reader at room temperature, because the luciferase activity at 37°C is only 10% of that observed at 20°C (Gorman et al., 2003). Intracellular ATP concentrations were measured by lysing the cells with in the same basal salt solution containing digitonin 300 μg/mL. A standard curve containing digitonin was used to calculte the ATP concentrations.

YO-PRO-1 uptake assay

YO-PRO-1 uptake was measured by fluorescence microscopy. BMDMs were seeded on coverslips and before the experiment were washed two times with basal salt solution. After that, 2 μM YO-PRO-1 was added to the assay media (saline solution) and the macrophages were treated with nigericin 25 μM. Images were acquired every 30 s at room temperature with a Nikon Eclipse Ti microscope using a 20x S Plan Fluor objective (numerical aperture 0.45), a digital Sight DS-QiMc camera (Nikon), 482nm/536nm filter set (Semrock) and NIS Elements software (Nikon). The fluorescence intensity related to basal were analyzed using ImageJ software (US National Institute of Health). Alternatively, YO-PRO-1 uptake was measured at room temperature using a Synergy *Neo*2 Hybrid Multimode plate reader (BioTek).

ELISA

IL-1β release was measured by ELISA for mouse IL-1β (R&D Systems) following the manufacturer's instructions and read in a Synergy Mx plate reader (BioTek). The concentration of IL-1β was estimated using a standard with known concentrations of recombinant IL-1β.

Lactate dehydrogenase (LDH) assay

LDH release was measured using the Cytotoxicity Detection kit (Roche) following the manufacturer's instructions, and expressed as percentage of total cell LDH content.

Monocyte migration assay

HEK-293T cells with an inducible system for GSDMD NT were seeded on 24-well plates at a density of $3x10^5$ cells by well. The next day the cells were incubated with 10 ng/mL doxycycline for 3 and 24 h in OptiMEM media. After this time, the supernatants were collected, centrifugated at 16,060 x*g* for 30 s and 500 μL of the free-cells supernatants were loaded into the lower chamber of a transwell insert (Sarstedt 83.3932.500_PET 5μm) placed on 24-well plate. At this point, 40 U/ml apyrase (Sigma-Aldrich) was added to the media of the well. In addition, the supernatant of HEK-293T cells with an inducible system for GSDMD NT not treated with doxycycline was supplemented with 10 ng/mL doxycycline to ensure that THP-1 chemotaxis is not due to the presence of doxycycline. After 30 min at 37°C, $3x10^5$ THP-1 cells were loaded into the upper chamber of the transwell inserts, and THP-1 cells were supplemented with 10 ng/mL doxycycline again to corroborate that the presence of doxycycline do not induce migration. After 3 or 24 h of incubation at 37°C, the inserts were removed and 16,000 units of flow cytometry counting beads (BD Trucount Tubes) were added per well. The migrated THP-1 with the counting beads were transferred to flow cytometry tubes. The samples were analyzed by flow cytometry (LSR Fortessa flow citometer, BD) recording events by gating on beads and collecting a fixed number of bead events per sample (730) and analyzed in FCS Express 5 Flow cytometry software (*De novo* Software). The percent of migration were calculated compared with total cells.

QUANTIFICATION AND STATISTICAL ANALYSIS

Statistical methods

The data are presented as the mean ± SEM. Data were analyzed using Prism Version 9.5.1 (GraphPad) software the non-parametric Mann-Whitney test (two tails, 95% confidence level), $*p < 0.05$; ns, not significant ($p > 0.05$) difference.